

Magnetism and the effect of anisotropy with a one-dimensional monatomic chain of cobalt using a Monte Carlo simulation

This article has been downloaded from IOPscience. Please scroll down to see the full text article.

2007 J. Phys.: Condens. Matter 19 446207

(<http://iopscience.iop.org/0953-8984/19/44/446207>)

View [the table of contents for this issue](#), or go to the [journal homepage](#) for more

Download details:

IP Address: 129.252.86.83

The article was downloaded on 29/05/2010 at 06:30

Please note that [terms and conditions apply](#).

Magnetism and the effect of anisotropy with a one-dimensional monatomic chain of cobalt using a Monte Carlo simulation

Lin He, Desheng Kong and Chinping Chen

Department of Physics, Peking University, Beijing 100871, People's Republic of China

E-mail: cpchen@pku.edu.cn

Received 27 June 2007, in final form 30 September 2007

Published 16 October 2007

Online at stacks.iop.org/JPhysCM/19/446207

Abstract

The magnetic properties of a one-dimensional (1D) monatomic chain of Co reported in a previous experimental work are investigated by a classical Monte Carlo simulation based on the anisotropic Heisenberg model. In our simulation, the effect of the on-site uniaxial anisotropy, K_u , on each individual Co atom and the nearest neighbour exchange interaction, J , are accounted for. The normalized coercivity $H_C(T)/H_C(T_{CL})$ is found to show a universal behaviour, $H_C(T)/H_C(T_{CL}) = h_0(e^{T_B/T} - e)$ in the temperature interval $T_{CL} < T \leq T_B^{Cal}$, arising from the thermal activation effect. In the above expression, h_0 is a constant, T_B^{Cal} is the blocking temperature determined by the calculation, and T_{CL} is the temperature above which the classical Monte Carlo simulation gives a good description of the investigated system. The present simulation has reproduced the experimental features, including the temperature dependent coercivity, $H_C(T)$, and the angular dependence of the remanent magnetization, $M_R(\theta, \phi)$, upon the relative orientation (θ, ϕ) of the applied field H . In addition, the calculation reveals that the ferromagnetic-like open hysteresis loop is a result of a slow dynamical process at $T < T_B^{Cal}$. The dependence of the dynamical T_B^{Cal} on the field sweeping rate R , the on-site anisotropy constant K_u , and the number of atoms in the atomic chain, N , has been investigated in detail.

(Some figures in this article are in colour only in the electronic version)

1. Introduction

One-dimensional (1D) spin lattice models have been studied in statistical physics for more than 80 years owing to a theoretical interest following the pioneer work of Ising [1]. The research interest of such systems lies in the physical properties, such as the phase transition, the dynamic process, etc, showing distinctive features from the bulk material. Relevant investigations

have their significances not only for phenomena with the 1D system but also for a better understanding of the properties of three-dimensional (3D) bulk material [2, 3]. One of the most important results obtained with these theoretical investigations is the Mermin–Wagner theorem stating that a long-range order of an infinite linear chain is absent at a finite temperature with a short-range exchange interaction (SREI) [4, 5].

Traditionally, a truly 1D system is untenable in experiment and thus bulk materials containing chain-like structure with strong magnetic intrachain interaction, J , along one direction are considered as a realizable 1D system [2]. Such a strong 1D magnetic intrachain coupling is usually produced by separating the chain-like structure with large nonmagnetic ions or complexes. The interchain interaction, J' , is therefore much weaker than the intrachain interaction, J , with these materials. Consequently, the properties arising from the 1D effect become significant only within the temperature interval $J'/k_B < T < J/k_B$, where k_B is the Boltzmann constant, and at $T \leq J'/k_B$, the 3D properties take over gradually [2]. For a 1D magnetic system realized with such a bulk material, it is usually considered as an infinite 1D chain. Long-range magnetic ordering is therefore not expected with such a system according to the Mermin–Wagner theorem. However, it is also possible to observe ferromagnetic (FM)-like properties, for example, an open hysteresis loop, in a slow dynamical process with these magnetic 1D systems [6] arising from the presence of a large uniaxial anisotropy. The possibility of generating 1D magnetic chains with long relaxation times at room temperature is very valuable for industrial applications and so relevant investigations have become an active research field [6].

An alternative approach to generating a 1D magnetic system has been made possible by the rapid advancements in material synthesis technology over the past few decades to artificially construct 1D chains on a nonmagnetic substrate [7–9]. Progress has been brought about by the work of Gambardella *et al*, reported recently [10]. They have fabricated a 1D Co chain with a length of 80 atoms arranged in parallel on a Pt (997) step edge. Two major magnetic properties have been observed experimentally, (a) the existence of an FM-like open hysteresis loop below the blocking temperature, $T_B^{\text{Exp}} = 15 \pm 5$ K, and (b) the angular dependence of the remanent magnetization, $M_R(\theta, \phi)$, upon the orientation of the applied field, H . This experimental result is unexpected by treating the 1D chain of 80 atoms as an infinite chain with a SREI in equilibrium, according to the Mermin–Wagner theorem [4, 5]. It is noted that the Mermin–Wagner theorem actually does not apply to a finite spin chain due to the lack of translational symmetry. Recently, Denisov and Hänggi [11] have studied a finite Ising spin chain with a nearest neighbour exchange interaction. They found that there exists a characteristic temperature below which a finite spin chain would exhibit an FM behaviour if the Ising spins are treated as an approximation of the classical Heisenberg spins with the presence of a very large uniaxial anisotropy potential between the two equilibrium states. Nevertheless, the natural characteristics of the open hysteresis loop as well as the remanent magnetization observed in the experiment are nonequilibrium phenomena involving a slow relaxation process [10]. Recently, Li and Liu have applied a kinetic Monte Carlo (KMC) method [12, 13] to investigate this 1D monatomic Co chain system. They have explicitly started with an anisotropic Heisenberg model and reduced it analytically to an Ising one subject to a potential barrier at the presence of a uniaxial anisotropy. The transition state of the spin flips between two metastable states owing to the presence of a potential barrier was accounted for. The numerical calculation by the KMC method was then performed. They have reproduced the FM feature of an open hysteresis loop at $T = 10$ K, and a superparamagnetic (SPM) behaviour at $T = 45$ K. According to the above analysis [11, 12], the presence of a potential barrier resulting from a large uniaxial anisotropy is essential to the existence of FM properties for the 1D monatomic chain of Co with a SREI.

In order to further understand the effect of anisotropy on the magnetization reversal of the 1D Co chain system in the experiment performed by Gambardella *et al* [10, 14–16], we have applied the classical MC method on the anisotropic Heisenberg model without resorting to the approximation to the Ising model in the presence of a large potential barrier, as carried out by Li *et al* [12]. The MC simulation adopts the standard Metropolis algorithm with a random updating scheme, see for example [17, 18]. This method has been applied to calculate the nonequilibrium dynamical phase transition properties of an anisotropic Heisenberg ferromagnet driven by an elliptically polarized magnetic field with success [19]. In our simulation, the numerical results have reproduced the magnetic behaviour of the 1D monatomic chain of Co observed in the experiment, including the M – H behaviour at $T = 10$ and 45 K and the angular dependence of the remanent magnetization, $M_R(\theta, \phi)$, upon the relative orientation of the applied field. Further calculations have revealed some interesting properties beyond the results obtained in the experiments [10] and in the calculations [12]. In particular, $H_C(T)$ measured along the axis of anisotropy can be described by the function $H_C(T)/H_C(T_{CL}) = h_0(e^{T_b/T} - e)$ within the temperature range, $T_{CL} < T \leq T_B^{\text{Cal}}$, where $T_B^{\text{Cal}}(N, R, K_u)$ is the blocking temperature depending on the number of atoms in the atomic chain, N , the field sweeping rate, R , and the anisotropy constant, K_u , and T_{CL} is the temperature limit above which the classical MC method describes the property of thermal activation properly. The dependence of T_B^{Cal} on N with a fixed K_u has been calculated also. The result explicitly demonstrates that T_B^{Cal} depends on the chain length with a small N and it approaches a constant value with N exceeding a critical value N_C .

2. Calculation procedure

The classical Heisenberg model with an on-site uniaxial anisotropy perpendicular to the chain axis was adopted to calculate the magnetic properties of the 1D chain. To conveniently describe the relative orientations of the physical quantities in the experiment by a Cartesian coordinate system, the plane of the Pt substrate is defined as the X – Y plane and the Co chain axis, along the X -axis. The easy axis, K_u , is then lying in the Y – Z plane with an inclination angle $\phi_K = 43^\circ$ from the Z -axis. The external field, H , can be applied in any relative orientation with respect to the axis of anisotropy, K_u . Its orientation is specified by (θ, ϕ) in which θ is the angular coordinate in the X – Z plane, and ϕ , in the Y – Z plane. The Z -axis is then specified as $(\theta = 0, \phi = 0)$. Thus, the Hamiltonian can be written as

$$E_H = - \sum_{\langle i, j \rangle} J \vec{S}_i \cdot \vec{S}_j - K_u \sum_i S_{iu}^2 - \mu \vec{H} \cdot \sum_i \vec{S}_i, \quad (1)$$

where the first term represents the FM exchange interaction with the constant coupling $J > 0$, the index $\langle i, j \rangle$ runs over all the pairs of nearest neighbour sites i and j , and S_i is the reduced spin variable at site i . The effective moment at each site for a Co atom is $\mu = 4\mu_B$. K_u is the uniaxial anisotropy constant representing the on-site anisotropy for each Co atom. With $K_u > 0$, the axis of anisotropy defines the orientation of the easy axis. S_{iu} is the projective component of the reduced spin variable along the uniaxial direction, and the applied magnetic field, H , is in units of Oe. In the calculation, each energy term, such as the anisotropy, magnetic energy, and thermal energy, is expressed in units of the exchange coupling strength, J . It is 7 meV determined in the experiment [10]. This value is obtained by rough estimation that is also adopted in the previous simulation [12]. Although in a recent investigation by a finite-size transfer matrix approach, the value of J is estimated differently as 20 meV [16], the result to describe the 1D monatomic chain of Co by the present simulation remains equally valid since it does not rely on the absolute value of J , which will be elaborated later.

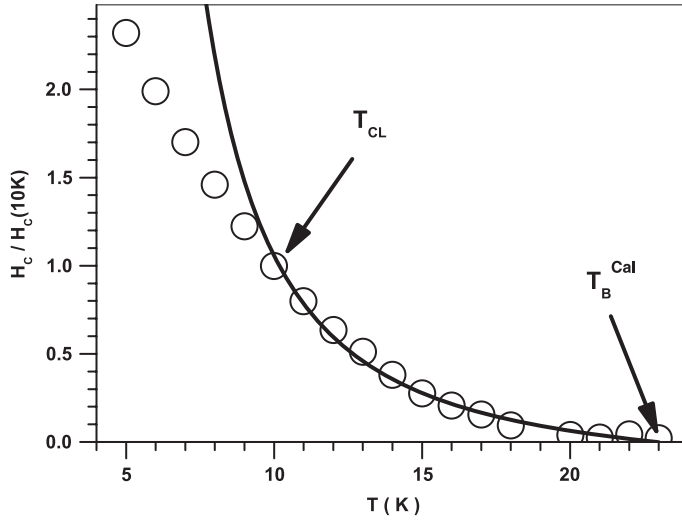


Figure 1. $H_C(T)$ determined from the $M-H$ loops calculated with the conditions, $N = 80$, $R = 2.67 \times 10^{-2}$ Oe/MCSS, $K_u = 0.3$, and $J = 7$ meV. It is normalized to the value calculated at $T = 10$ K, i.e. $H_C(10 \text{ K}) = 17$ kOe.

To generate a trial spin configuration with one MC step, a spin is randomly chosen and then flipped towards an arbitrary orientation with a probability, $p = \text{Min}\{1, \exp(-\Delta E_H/k_B T)\}$, where the function, Min, is to pick the smallest value in the argument, ΔE_H is the change in energy owing to the reorientation of the spin at temperature, T . The computational time unit, t_C , for the simulation is then defined by the MC step per site (MCSS). For a chain of N atoms, there are N steps of MC calculation in one MCSS. For a data point in the hysteresis loop, the value of magnetization has been averaged over 200 independent runs to reduce the level of fluctuation.

3. Results and discussion

$M-H$ curves are calculated for the monatomic chain of Co with different parameters of N , R , and K_u , at various temperatures. The temperature dependent coercivity, $H_C(T)$, and the corresponding blocking temperature, T_B^{Cal} , are obtained corresponding to these various conditions. It is found that $H_C(T)$ follows a universal behaviour, $H_C(T)/H_C(T_{\text{CL}}) = h_0(e^{T_B/T} - e)$ with $T_{\text{CL}} < T < T_B^{\text{Cal}}$. The experimentally observed results reported in [10], i.e. the temperature dependent coercivity, $H_C(T)$, and the angular dependence of the remanent magnetization, $M_R(\theta, \phi)$, are then reproduced by the present calculation method. The effect of the anisotropy and the atomic chain length on the blocking temperature is then assessed in detail.

3.1. Temperature dependent coercivity $H_C(T)$ and blocking temperature

For the atomic chain with experimental parameters of $N = 80$, $K_u = 0.3$, and $J = 7$ meV, the $M-H$ curves at different temperatures have been calculated at the field sweeping rate of $R = 2.67 \times 10^{-2}$ Oe/MCSS. The temperature dependent coercivity $H_C(T)$ determined from these calculated loops is presented in figure 1. It is normalized to the coercivity at $T = 10$ K, $H_C(10 \text{ K}) \sim 17$ kOe. Taking into account the thermal activation effect, the coercivity is expected to decrease exponentially with increasing temperature, i.e. $H_C(T) \sim e^{T_B/T}$, and vanishes at the blocking temperature, $T_B = T_B^{\text{Cal}}$. The solid curve in figure 1 is a fitting result using the function

$$H_C(T)/H_C(T_{\text{CL}}) = h_0(e^{T_B/T} - e), \quad (2)$$

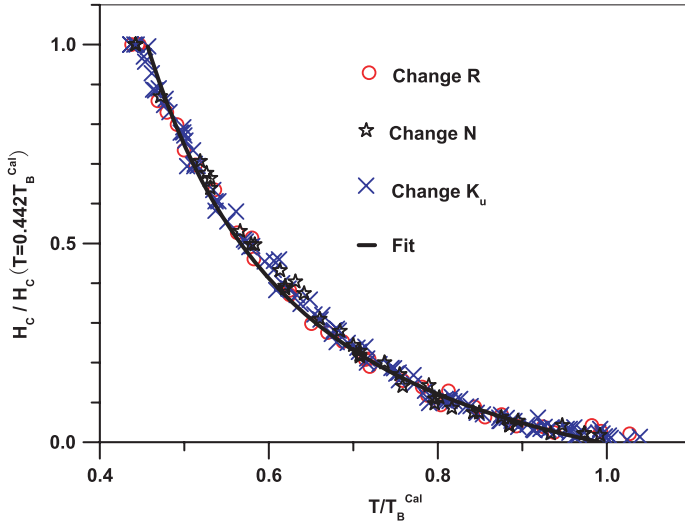


Figure 2. $H_C(T)$ normalized over the coercivity at $T = 0.442T_B^{\text{Cal}}$, $H_C(0.442T_B^{\text{Cal}})$, versus the reduced temperature, T/T_B^{Cal} with one of the parameters, N , V , and K_u in variation. The solid curve is for the fitting results by equation (2).

where h_0 is a constant and the exponential constant e is obtained from the condition, $H_C(T_B^{\text{Cal}}) = 0$. The blocking temperature determined by the fitting is $T_B^{\text{Cal}} \sim 22.6$ K. It is higher than the experimental value, $\sim 15 \pm 5$ K, attributed to the faster field sweeping rate in the calculation.

Equation (2) reflects the thermal activation effect according to the Arrhenius law. It is expected as a direct consequence from the model adopted in the calculation. For the reorientation of a spin at temperature, T , the probability is modelled as $p = \text{Min}\{1, \exp(-\Delta E_H/k_B T)\}$, with ΔE_H , the change in energy owing to the spin flip. By treating ΔE_H as the energy barrier E_a , the time needed for the spin flip is, $t \propto 1/p \propto \exp(E_a/k_B T)$. Since $H_C(T) \propto t(T)$, and at $T = T_B$, the blocking effect is expected to vanish due to the activation of thermal energy, $k_B T_B \sim E_a$, we have $H_C(T) \propto (e^{T_B/T} - e)$. By accounting for the fact that the above property is valid at $T > T_{\text{CL}}$ due to the limitation of the calculation elaborated below, equation (2) is thus obtained. Equation (2) is not applicable in the temperature range $T < T_{\text{CL}} = 0.442T_B^{\text{Cal}}$. For a system with a magnetic potential barrier E_a which obstructs the magnetization reversal, the ratio, $E_a/k_B T$, determines the switching rate of the spins over the barrier subject to the thermal activation effect described by the Arrhenius law. However, Wernsdorfer *et al*, have shown clearly with an experiment that, as the magnitude of $E_a/k_B T$ reaches 58.8, the quantum tunnelling rate of the spins will become comparable to that of the thermal activation for the 1D magnetic system in their experiment [20]. To avoid such a possible quantum effect which is beyond the description of the classical MC simulation, we applied the simulation only within the temperature region of $0.442T_B^{\text{Cal}} < T < T_B^{\text{Cal}}$ in the following presented calculations.

Since T_B^{Cal} depends on N , R , and K_u , it is necessary to investigate its dependence on these parameters in order to understand the magnetization reversal behaviour or the property of $H_C(T)$. Figure 2 shows the temperature dependent coercivity in the temperature interval $0.442T_B^{\text{Cal}} < T < T_B^{\text{Cal}}$ obtained by (a) increasing R from 2×10^{-3} Oe/MCSS to 1.34 Oe/MCSS with $N = 80$ and $K_u = 0.3J$, (b) varying N from 10 to 240 atoms with $K_u = 0.3J = 2.1$ meV and $R = 2.67 \times 10^{-2}$ Oe/MCSS, and (c) varying K_u from 0.1 to 1.32J by fixing $N = 80$ atoms and $R = 2.67 \times 10^{-2}$ Oe/MCSS. The coercivity thus calculated is then normalized over the value of H_C at $T = 0.442T_B^{\text{Cal}}$ and plotted versus the reduced temperature $\tau = T/T_B^{\text{Cal}}$. As expected, these data reveal a universal behaviour. They

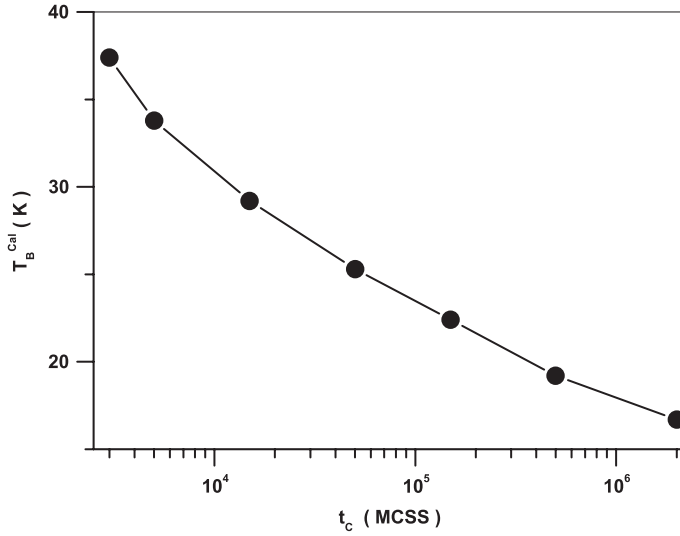


Figure 3. Blocking temperatures T_B^{Cal} versus the computer calculation time, t_c . The solid curve is plotted to guide the eyes.

collapse on a single curve. It indicates that the physical process manifested in the temperature variation effect for the spin chain is, indeed, the thermal activation against the anisotropy potential barrier. The fitting result of equation (2) is also plotted in figure 2 by the solid curve. In the temperature interval $0.442T_B^{\text{Cal}} < T < T_B^{\text{Cal}}$, equation (2) gives a good description of the result of our calculation. With this universal behaviour, the blocking temperature can be uniquely determined, corresponding to specified V , K_u , and N parameters.

Figure 3 shows T_B^{Cal} determined from the calculated $M-H$ loop versus the computer calculation time, t_c , needed for sweeping a complete $M-H$ loop, which is in units of MCSS. The solid curve connecting the ‘data’ points in figure 3 is a guide for the eyes. For a slow relaxation process, it is expected that the system relaxes exponentially with physical time, i.e. it shows a linear behaviour in the $\log(t)$ plot. Although t_c is not linearly proportional to the physical time [21–23], the calculated blocking temperature T_B^{Cal} versus t_c still exhibits a behaviour close to an exponential relaxation process, i.e. close to a linear relation in the $\log(t_c)$ plot, as shown by figure 3. This apparent higher order effect deviating from the logarithmically exponential relaxation with the computer timescale probably arises from the nonlinear conversion relation from the computer calculation time to the physical timescales. Without affecting the conclusion in the present work, the computer calculation timescale is adopted. By increasing the field sweeping time duration for a complete $M-H$ loop from 3×10^3 MCSS to 2×10^6 MCSS, corresponding to reducing the field sweeping rate from 1.34 Oe/MCSS to 2×10^{-3} Oe/MCSS, the blocking temperature then decreases from 37.4 to 16.7 K. The dependence of the coercivity, hence, the blocking temperature T_B^{Cal} , upon the field sweeping rate, R , indicates that the calculated FM property at $T < T_B^{\text{Cal}}$ is not for an equilibrium state. The occurrence of a finite-area hysteresis, which is calculated based on the model of a 1D atomic chain with SREI, does not conflict with the Mermin–Wagner theorem since the calculated hysteresis loop is not for a true FM property with a long-range order in thermodynamic equilibrium.

3.2. Angular dependent hysteresis loops and remanent magnetization, $M_R(\theta, \phi)$

Experimentally, the coercivity and the blocking temperature of the 1D system also depend on the measured time or the field sweeping rate [20]. For a comparison with the results reported

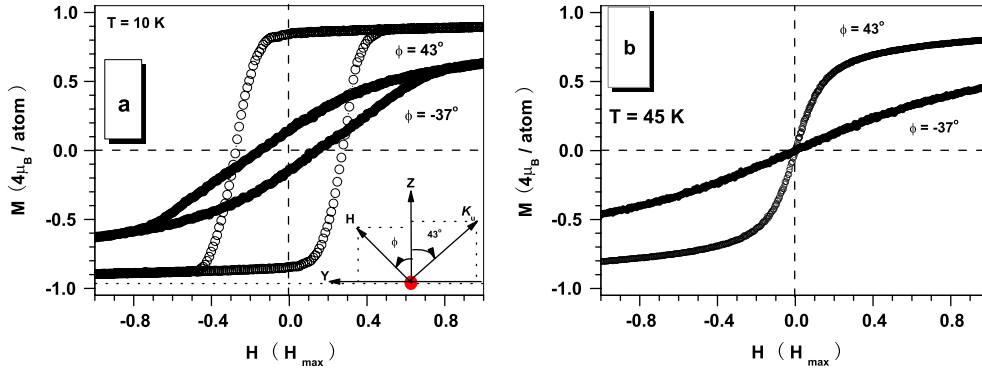


Figure 4. M - H curves calculated for the 1D monatomic chain with $N = 80$ atoms. The magnetization M is expressed in units of $4\mu_B/\text{atom}$. The applied field is expressed in units of the maximum sweeping limit, H_{max} , in the calculation. (a) M - H curves at $T = 10$ K. $H_{\text{max}} = 120$ kOe. The lower right quarter shows a simple depiction for the relative orientations of the monatomic chain axis, the anisotropy axis, the applied field direction, and the coordinate axes. (b) The curves calculated at $T = 45$ K. $H_{\text{max}} = 600$ kOe.

in the experiment, M - H curves at $T = 10$ and 45 K are calculated in the present work with $N = 80$ atoms, $K_u = 0.3J = 2.1$ meV, and $R = 2.67 \times 10^{-2}$ Oe/MCSSS, as shown in figure 4. The magnetization M is expressed in units of $4\mu_B/\text{atom}$ in both figures 4(a) and (b) while the applied field H , in units of H_{max} , which is 120 kOe in figure 4(a) and 600 kOe in figure 4(b). The calculations have reproduced the major features of the M - H loops observed in the experiment, i.e. an open hysteresis loop at $T = 10$ K and an SPM behaviour at $T = 45$ K. In addition, the remanent magnetizations $M_R(\theta, \phi)$ determined from the calculated loops at $T = 10$ K exhibit the same angular dependence on θ and ϕ as observed in the experiment. All the calculated magnetizations are expressed in units of $4\mu_B/\text{atom}$.

To clearly reveal the details in calculating the M - H curves for the monatomic chain, the relevant axes are depicted in a simple diagram shown in the lower right quarter of figure 4(a). From the depiction, the Y - Z plane is lying in the plane of the figure with the positive Y directed to the left and the positive Z upwards. The axis of the 1D chain is along the X -axis whose positive direction points into the plane of the figure. According to the experiment, the easy axis of anisotropy, K_u , lies in the Y - Z plane with an inclination, $\phi_K = 43^\circ$, from the Z -axis. The M - H curves shown in figure 4(a) for $T = 10$ K and figure 4(b) for $T = 45$ K are calculated using the experimental conditions, i.e. the field is applied along the easy axis with $\phi = \phi_K = 43^\circ$, and at 80° away from the easy axis with $\phi = -37^\circ$. At $T = 10$ K, both of the calculated curves exhibit open hysteresis loops. As the temperature rises to $T = 45$ K, the M - H curves reveal the property of superparamagnetism, see figure 4(b). These reproduce the experimental features [10].

A further investigation by calculation on the remanent magnetization, $M_R(\theta, \phi)$, is performed at $T = 10$ K. In the experiment, $M_R(\theta, \phi)$ is the magnetization measured by a small field after the magnetizing field, which drives the sample to saturation, is removed [10]. It is actually the remanent magnetization in a M - H measurement. Its magnitude depends on the orientation (θ, ϕ) of the sweeping applied field. In figure 5(a), ϕ is defined with the same meaning as in figure 4(a) and θ is defined as the inclination angle from the Z -axis in the X - Z plane as shown by the depiction in figure 5(b). The remanent magnetization, $M_R(\theta, \phi)$, versus the inclination angle, ϕ , in the Y - Z plane is determined from a series of calculated M - H curves and plotted in figure 5(a) by the solid circles. Similarly, the calculated

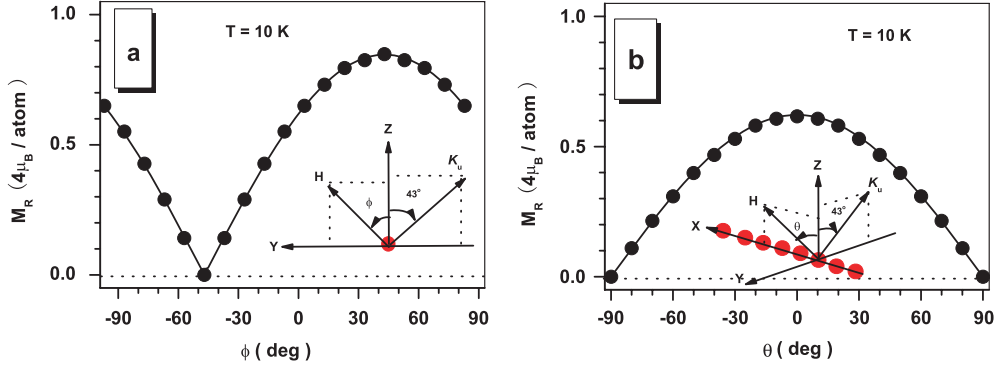


Figure 5. Remanent magnetization, $M_R(\theta, \phi)$, versus the orientation of the applied field at $T = 10$ K. M_R is expressed in units of $4\mu_B/\text{atom}$. (a) M_R versus ϕ , with $\theta = 0^\circ$. (b) M_R versus θ with $\phi = 0^\circ$. The solid curves in (a) and (b) are the fitting results of $|\cos(\phi - 43^\circ)|$ and $|\cos(\theta)|$, respectively.

M_R versus θ is presented in figure 5(b). The solid curve in figures 5(a) and (b) are for the function $g(\phi) = |\cos(\phi - \phi_K)|$ and $f(\theta) = |\cos(\theta)|$, respectively, which are determined in the experiment by fitting the measured remanent magnetization. The calculated M_R at $T = 10$ K, as shown in figure 5, describes well the angular dependent property of M_R measured in the experiment [10]. Interestingly, even at temperature as low as 10 K, H_C and M_R are zero and the chain shows SPM behaviour with the applied field H exactly perpendicular to the easy axis, K_u , according to the present calculation. This is mainly due to the absence of an anisotropy component within the plane of the sweeping field, i.e. without an anisotropy barrier to obstruct the magnetization reversal process. A similar property is also observed with a FM material with large anisotropy, for example, for a FM nanowire with large shape anisotropy along the axis of the wire, H_C and M_R are also much reduced with the applied field H perpendicular to the easy axis [24].

3.3. The dependence of blocking temperature on anisotropy constant and chain length

Figure 6 shows T_B^{Cal} versus the magnitude of the anisotropy constant, K_u at a field sweeping rate of $R = 2.67 \times 10^{-2}$ Oe/MCSS. The solid circle is for $K_u = 2.1$ meV = $0.3J$, which is the same as that in the experiment [10], and the solid triangle, $K_u = 9.3$ meV = $1.32J$, which is for the upper limit of anisotropy with a single Co atom on Pt (997) [14]. According to the analysis by Li *et al* [12], the potential barrier in the anisotropic Heisenberg model can be approximated by the expression, $E_a = [2K_u + (\sum_j JS_j + \mu H)S_i]^2 / 4K_u$. This energy barrier depends not only on the anisotropy constant K_u but also on the exchange coupling strength J and the chain length, N . The barrier height increases with increasing anisotropy when $K_u > \frac{1}{4}(\sum_j JS_j + \mu H)S_i$. In the limit $K_u \gg \frac{1}{4}(\sum_j JS_j + \mu H)S_i$, E_a is expected to increase linearly with the magnitude of K_u . This is consistent with our result by a direct MC calculation. The increase of T_B^{Cal} with K_u is linear as $K_u > 0.3J$.

Figure 7 shows the dependence of T_B^{Cal} on N for the monatomic chain with $K_u = 0.3J$ and $R = 2.67 \times 10^{-2}$ Oe/MCSS. It reveals that T_B^{Cal} increases with N , and then becomes almost a constant after reaching 80 atoms. In a previous numerical investigation on a classical spin chain with similar Hamiltonian to our model, three magnetization reversal modes have been proposed for the 1D system [25]. As the length of the spin chain increases from several spins to hundreds of spins, the reversal modes change from coherent rotation, in

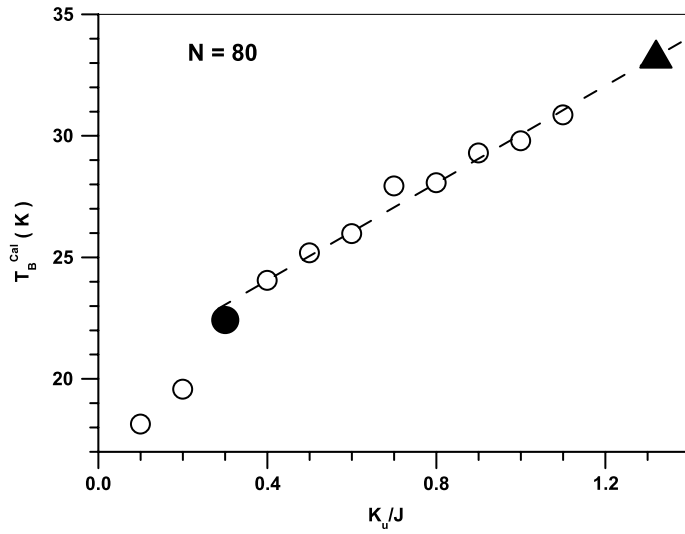


Figure 6. Blocking temperatures T_B^{Cal} versus the anisotropy constant, K_u . The field sweeping rate is $R = 2.67 \times 10^{-2}$ Oe/MCSS.

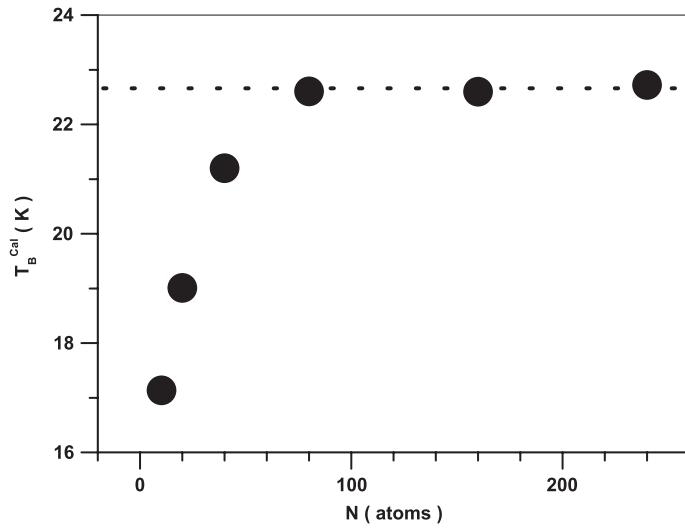


Figure 7. Dependence of T_B^{Cal} on the number of atoms, N , calculated with $K_u = 0.3J$. The field sweeping rate is $R = 2.67 \times 10^{-2}$ Oe/MCSS.

which all the spins in the chain rotate coherently, to the soliton–antisoliton nucleation mode, in which the magnetization reversal proceeds with the spins splitting into two parts with opposite direction of magnetization reversal, and finally to the multidroplet nucleation mode with which many nuclei appear at the same time and then join each other, leading to a complete magnetization reversal. In our simulations, we observe the reversal process by coherent rotation in the small size limit of the monatomic chain. By increasing the chain length, the magnetization reversal of the chain proceeds more often by the soliton–antisoliton nucleation mode in a series of repeated calculations using the same condition. As the chain length further increases, exceeding the critical value of 80 atoms, the reversal is always by multidroplet nucleation mode which is similar to the reversal mode of an infinite chain. Thus, T_B becomes almost independent of the number of atoms with $N > 80$, as shown in figure 7. According to the present calculation, before N approaches the critical value for the multidroplet nucleation mode, the reversal process shows a property of bistability either with the coherent

rotation or the soliton–antisoliton nucleation, and T_B is obtained as a result of statistical average.

4. Conclusion

In conclusion, we have calculated the magnetic properties of a 1D monatomic chain of Co by a classical MC calculation based on the anisotropic Heisenberg model. The temperature dependence of the coercivity, $H_C(T)$, and the angular dependence of the remanent magnetization, $M_R(\theta, \phi)$, upon the applied field direction are in agreement with the previously reported experiment. The calculation is demonstrated as a proper technique to calculate the properties of a 1D spin chain with a slow relaxation process. It is apparent that the potential barrier obstructing the spin reversal is a crucial factor, resulting in an FM-like $M-H$ behaviour for the 1D monatomic chain at low temperature. Additionally, the calculation result does not conflict with the traditional 1D spin lattice theory with SREI [1, 4, 5]. This can be well described by the statement put forward by Jacobs and Bean [26] ‘... the one-dimensional Ising chain (or any anisotropic chain) is not ferromagnetic in equilibrium but will, in fact, show all the usual characteristics of ferromagnetic matter owing to the difficulty of reaching equilibrium.’

References

- [1] Ising E 1925 *Z. Phys.* **31** 253
- [2] Steiner M, Villian J and Windsor C G 1976 *Adv. Phys.* **25** 87
- [3] Steiner M and Mykeska H J 1991 *Adv. Phys.* **40** 191
- [4] Landau L D and Lifshitz E M 1959 *Statistical Physics* vol 5 (London: Pergamon) p 482
- [5] Mermin N D and Wagner H 1966 *Phys. Rev. Lett.* **17** 1133
- [6] Coulon C, Miyasaka H and Clerac R 2006 *Struct. Bond.* **122** 163
- [7] Elmers H J, Hauschild J, Hoche H, Gradmann U, Bethge H, Heuer D and Kohler U 1994 *Phys. Rev. Lett.* **73** 898
- [8] Shen J, Skomski R, Klaua M, Jenniches H, Manoharan S S and Kirschner J 1997 *Phys. Rev. B* **56** 2340
- [9] Hauschild J, Elmers H J and Gradmann U 1998 *Phys. Rev. B* **57** R677
- [10] Gambardella P, Dallmeyer A, Maiti K, Malagoli M C, Eberhardt W, Kern K and Carbone C 2002 *Nature* **416** 301
- [11] Denisov S I and Hänggi P 2005 *Phys. Rev. E* **71** 046137
- [12] Li Y and Liu B-G 2006 *Phys. Rev. B* **73** 174418
- [13] Li Y and Liu B-G 2006 *Phys. Rev. Lett.* **96** 217201
- [14] Gambardella P, Rusponi S, Veronese M, Dhessi S S, Grazioli C, Dallmeyer A, Cabria I, Zeller R, Dederichs P H, Kern K, Carbone C and Brune H 2003 *Science* **300** 1130
- [15] Gambardella P, Dallmeyer A, Maiti K, Malagoli M C, Rusponi S, Ohresser P, Eberhardt W, Carbone C and Kern K 2004 *Phys. Rev. Lett.* **93** 077203
- [16] Vindigni A, Rettori A, Pini M G, Carbone C and Gambardella P 2006 *Appl. Phys. A* **82** 385
- [17] Acharyya M 2004 *Phys. Rev. E* **69** 027105
- [18] Binder K and Heermann D W 1997 *Monte Carlo Simulation in Statistical Physics (Springer Series in Solid-State Sciences)* (New York: Springer)
- [19] Hinzke D and Nowak U 1998 *Phys. Rev. B* **58** 265
- [20] Wernsdorfer W, Clérac R, Coulon C, Lecren L and Miyasaka H 2005 *Phys. Rev. Lett.* **95** 237203
- [21] Sampaio L C, Hyndman R, de Menezes F S, Jamet J P, Meyer P, Gierak J, Chappert C, Mathet V and Ferre J 2001 *Phys. Rev. B* **64** 184440
- [22] Nowak U, Chantrell R W and Kennedy E C 2000 *Phys. Rev. Lett.* **84** 163
- [23] Cheng X Z, Jalil M B A, Lee H K and Okabe Y 2006 *Phys. Rev. Lett.* **96** 067208
- [24] Sellmyer D J, Zheng M and Skomski R 2001 *J. Phys.: Condens. Matter* **13** R433
- [25] Hinzke D and Nowak U 2000 *Phys. Rev. B* **61** 6734
- [26] Jacobs I S and Bean C P 1963 *Magnetism* vol 3, ed T Rado George and S Harry (New York: Academic) p 300